Chemical Engineering Journal 160 (2010) 408–416

Contents lists available at ScienceDirect

Chemical Engineering Journal

journal homepage: www.elsevier.com/locate/cej

Equilibrium two-parameter isotherms of acid dyes sorption by activated carbons: Study of residual errors

Mahdi Hadi [a], Mohammad R. Samarghandi [a], Gordon McKay [b,*]

[a] Department of Environmental Health Engineering, School of Public Health, Center for Health Research, Hamadan University of Medical Sciences, Hamadan, Iran
[b] Department of Chemical and Biomolecular Engineering, Hong Kong University of Science and Technology, Clearwater Bay, Kowloon, Hong Kong SAR

ARTICLE INFO

Article history:
Received 28 September 2009
Received in revised form 2 March 2010
Accepted 4 March 2010

Keywords:
Adsorption
Active carbons
Isotherms
Acid dyes
Error function analysis

ABSTRACT

The adsorption of two acid dyes Acid Black 1 (AB1) and Acid Blue 113 (AB113) onto mesoporous granular pine-cone derived activated carbon and the adsorption of three acid dyes Acid Black 80 (AB80), Acid Red 114 (AR114) and Acid Yellow 117 (AY117) onto microporous Granular Activated Carbon (GAC) type F400, from aqueous solution, has been studied in a batch system. Seven two-parameter isotherm models – Langmuir, Freundlich, Dubinin–Radushkevich, Temkin, Halsey, Jovanovic and Harkins–Jura – were used to correlate the experimental data. Adsorption isotherm modeling shows that the interaction of dye with activated carbon surface is by localized monolayer adsorption. In order to determine the best fit isotherm for each system, nine error analysis methods, namely, chi-square (χ^2), log-likelihood (G^2), residual root mean square error (RMSE), sum of the squares of the errors (ERRSQ), composite functional error (HYBRD), derivative of Marquardt's percent standard deviation (MPSD), average relative error (ARE), sum of absolute error (EABS) and average percentage error (APE) were used to evaluate the data.

In order to facilitate decision making for the best fit data set, a procedure of normalizing and combining the error results was adopted producing a "sum of the normalized errors" for each parameter set from which the "lowest normalized error set" is selected.

1. Introduction

In general, there are four main methods of reducing color in textile effluent streams: physical methods such as membrane technology, chemical methods such as coagulation and photochemical oxidation processes, biological methods such as anaerobic/aerobic sequential process and physico-chemical processes [1,2]. Among the physico-chemical processes, adsorption technology is considered to be one of the most effective and proven technologies having potential application in both water and wastewater treatment [3].

Adsorption equilibria data is the most important piece of information in understanding an adsorption process. No matter how many components are present in the system, the adsorption equilibria and diffusion of pure components are the essential ingredient for understanding the amount of those components which can be accommodated by a solid adsorbent [4,5].

Modeling of sorption isotherm data is important for predicting and comparing adsorption performance. Two-parameter isotherm models are available for modeling adsorption data. Freundlich [6] and Langmuir [7] models are the most commonly used isotherms. Furthermore, other two-parameter models such as Temkin [8], Dubinin [9], Jovanovic [10], Halsey [11] and Harkins–Jura [12] were also used.

Activated carbon is the most commonly used adsorbent of dye removal by adsorption [13]. Although commercial activated carbon is a preferred adsorbent for color removal, its widespread use is restricted due to high cost. As such, alternative non-conventional adsorbents have been investigated. It is well known that natural materials, waste materials from industry and agriculture and biosorbents can be obtained and employed as inexpensive adsorbents [14,15].

Many investigations have studied the feasibility of using inexpensive alternative materials like bagasse [16], wood [17], tree fern [18], sugarcane dust [19], orange peel [20], peat [21] and chitin [22] as carbonaceous precursors for the dye removal.

Pine is a suitable tree for decorative planting in parks and is used usually as a decorative plant in national parks. Thus ground pine-cone may be abundantly available and, it would be worthwhile to develop a low-cost adsorbent from this waste material which may also be regarded as a sustainable resource, since the trees themselves do not have to be harvested. However, the abundant supply of ground pine-cone as a waste from national parks makes production of activated carbon from this material more financially viable

* Corresponding author at: Department of Chemical and Biomolecular Engineering, Hong Kong University of Science and Technology, Clearwater Bay, New Territory, Hong Kong SAR. Tel.: +852 2358 8412; fax: +852 2358 0054.
E-mail address: kemckayg@ust.hk (G. McKay).

1385-8947/$ – see front matter © 2010 Elsevier B.V. All rights reserved.
doi:10.1016/j.cej.2010.03.016

Nomenclature

C_e	Equilibrium concentration of dye in solution ($mg\,L^{-1}$)
C_0	Initial dye concentration ($mg\,L^{-1}$)
m	Sorbent mass (g)
V	The solution volume (L)
q_e	Amount of dye adsorbed at equilibrium time ($mg\,g^{-1}$)
q_m	Maximum adsorption capacity in Langmuir model ($mg\,g^{-1}$)
b	Langmuir constant related to the energy of adsorption ($L\,mg^{-1}$)
n	Freundlich and Halsey equation exponents
K_f	Freundlich constant indicative of the relative adsorption capacity of the adsorbent ($mg^{1-1/n}\,L^{1/n}\,g^{-1}$)
R	Universal gas constant ($kJ\,mol^{-1}\,K^{-1}$)
T	Temperature (K)
b_T	Temkin constant related to heat of sorption ($kJ\,mol^{-1}$)
K_T	Temkin equilibrium isotherm constant ($L\,g^{-1}$)
K_j	Jovanovic isotherm constant ($L\,g^{-1}$)
q_{mj}	Maximum adsorption capacity in Jovanovic model ($mg\,g^{-1}$)
Q_s	Theoretical monolayer saturation capacity in Dubinin–Radushkevich model ($mg\,g^{-1}$)
B_D	Dubinin–Radushkevich model constant ($mol^2\,kJ^{-2}$)
ε	Polanyi potential
A_H	Harkins–Jura isotherm parameter
B_2	Harkins–Jura isotherm constant
K_H	Halsey isotherm constant
N	Number of experimental points
GPAC	Granular pine-cone derived activated carbon

since using grain or coal as raw materials for activated carbon will require extra capital for procurement.

The present research aims to test several two-parameter isotherm models to describe the sorption data generated from acid dyes sorption by two-type activated carbons (pine-cone derived activated carbon, GPAC, and commercial activated carbon, F400). The isotherm models parameters were determined using the trial-and-error non-linear method by OriginPro Software. Nine error functions were also used as a measure of the differences between values predicted by a model and the values actually observed from the experimental data being modeled.

2. Materials and methods

2.1. Facilities

Weighing of materials was performed by using an analytical balance with precision of ±0.0001 g (model Sartorius ED124S). Drying of materials was carried out in an electric oven (model PARS TEB). Carbonization was carried out in a muffle furnace (model Exiton). The pH of solutions was measured using a digital pH-meter (model Sartorius Professional Meter PP-50). The dye solutions were stirred using an inductive stirring system (Oxitop IS 12) within a WTW-TS 606/2-i incubator. The samples were centrifuged using a 301 Sigma Centrifuge. The dye concentration in the samples was measured spectrophotometrically, using a UV-1700 Pharmaspec Shimadzo spectrophotometer.

Table 1
Information regarding the acid dyes.

	Name of dyes				
	AB1	AB113	AB80	AR114	AY117
Color index number	20,470	26,360	61,585	23,635	24,820
Molecular mass (g)	618	681	676	830	848
λ_{max} (nm)	622	574	626	522	438

2.2. Raw materials

Dried pine-cone was used as the raw material to produce the adsorbent. The pine-cones were collected from the Mardom Park in front of Hamadan University of Medical Sciences of Iran. The ground pine-cone derived activated carbon (GPAC) is advantageous over carbons made from other materials because of its high density and high purity. This carbon is harder and more resistant to attrition. Acid Blue 113 (AB113) one disazo type dye and Acid Black 1 (AB1), a sulfonated azo dye were used in this study. AB113 and AB1 dyes were obtained from Alvansabet dyestuff and textile auxiliary manufacturer company in the west of Iran.

Three other dyes, namely Acid Blue 80 (AB80), Acid Red 114 (AR114) and Acid Yellow 117 (AY117), were also used in this study. The dyestuffs were used as the commercial salts. AB80 and AY117 were supplied by Ciba Speciality Chemicals and AR114 was supplied by Sigma–Aldrich Chemical Company [23]. Some information regarding the five acid dyes, which were used to measure and prepare standard concentration dye solutions, is listed in Table 1. The data include color index number, molecular mass and the wavelengths at which maximum absorption of light occurs, λ_{max}. The structures of the five acid dyes are shown in Appendix A Supplementary material.

2.3. Adsorbents

2.3.1. Pine-cone derived activated carbon

The local granular activated carbon (GPAC) was derived from the ground pine-cone. The local GAC was produced by exposing the raw pine-cones to a thermal-chemical process. First of all the pine-cones were crushed and washed with hot water and then dried at 100 °C in an oven overnight. A 50 g crushed sample was mixed with a pre-determined volume of phosphoric acid with concentration of 95% in the mass ratio of 1:10. This mixture was transferred to a stainless steel tube (50 mm diameter and 250 mm long). This tube was inserted to a muffle furnace, which was programmed to gradually reach up to 900 °C within 3 h, this temperature was maintained for 1 h, and then gradually cooled down to the room temperature. The end product was repeatedly washed using hot distilled water until the washings showed pH > 6.9; the washed sample was then again dried at 120 °C in an oven overnight. The final sample was then ground in a household-type blender and passed through a series of sieves (20, 30, 40, 50 U.S. Standard mesh sizes). A mixture of the residuals on 30, 40 and 50 sieves were kept in an air-tight bottle and used as the adsorbent in this study. The average adsorbent particle size was 0.5 mm.

The specific surface area of local GPAC was obtained by the determination of the optimal concentration of methylene blue dye adsorbed onto the GPAC sorbent at constant temperature 20 °C. Adsorption tests of methylene blue on prepared activated carbon were examined using a batch process by mixing 0.3 g of adsorbent in stoppered conical flasks with 100 ml of methylene blue solutions of concentration ranging from 100 to 1000 $mg\,L^{-1}$ at a pH of 7.5 ± 0.2. For the all the concentration range studied (100–1000 $mg\,L^{-1}$), the mixture was magnetically stirred at a constant revolution for 3 days which is more than sufficient time to reach equilibrium. Absorbance measurements were performed on

Table 2
Physical properties of activated carbon F400.

Total surface (N_2 BET method) ($m^2\,g^{-1}$)	1150
Bed density, backwashed and drained ($\times 10^3\,kg\,m^{-3}$)	425
Particle density ($g\,cm^{-3}$)	1.30
Particle voidage fraction	0.38

methylene blue solutions at 660 nm to determine the equilibrium concentration. The methylene blue calculated surface area was $734\,m^2\,g^{-1}$.

The potential capacity of an adsorbent for adsorption can be evaluated through iodine adsorption from aqueous solutions using test conditions referred to as the Iodine Number determination. This indicates the relative activation level and the micropore surface area available. Usually adsorbents with a high Iodine Number have a high surface area and are suitable for adsorbing small compounds [24]. The Iodine Number was measured according to the standard procedure [25] by using the 0.1 N standardized iodine solution. Sample volumes of 100 ml of the iodine solution were treated with 0.6, 0.9, and 1.2 g of the different samples. After equilibrium, the remaining iodine in the supernatants was titrated with 0.1 N sodium thiosulfate solution. The Iodine Number was reported as the amount of iodine adsorbed per gram of adsorbent at a residual iodine concentration of 0.02 N. The calculated Iodine Number value was $483.5\,mg\,g^{-1}$.

The apparent density was calculated by filling a calibrated cylinder with a given activated carbon weight and tapping the cylinder until a minimum volume was recorded. This density was referred as tapping or bulk density of adsorbent. For the real density a pycnometer method was used, which consisted of filling a pycnometer with the activated carbon, then added a solvent (methanol) to fill the void, at each step the weight was determined. The apparent and real density values were equal to 0.50 and $1.70\,g\,cm^{-3}$, respectively.

The pore volume and the porosity were determined by using a volumetric method which consists in filling a calibrated cylinder with a V_1 volume of activated carbon (mass m_1) and solvent (methanol) until volume V_2 (total mass m_2) is reached. Knowing the density of solvent, total porosity volume ($1.40\,cm^3\,g^{-1}$) and the porosity (70%) of the adsorbent were easily calculated. The BET nitrogen surface area was determined to be $869\,m^2\,g^{-1}$.

2.3.2. Activated carbon F400

The other adsorbent used in the research was a Granular Activated Carbon (GAC) type F400; it was supplied by Chemviron Carbon Ltd. Table 2 shows the physical properties of Activated Carbon F400. This carbon was described by the supplier as a generally effective water treatment activated carbon. Activated Carbon Filtrasorb 400 was crushed by using a hammer mill and washed with distilled water to remove fines. It was dried at 110 °C in an oven for 24 h and then sieved into several discrete particle size ranges, namely, 200–355, 355–500, 500–710 and 710–1000 μm. The 500–710 μm size range activated carbon was used for the experiments in this study. The carbon particles were assumed to be spheres having a diameter given by the arithmetic mean value between respective mesh sizes (average particle diameter, d_p, was 605 μm) [23]. The carbon properties are shown in Table 2.

2.4. Dye concentration measurement and equilibrium experiment

An accurately weighed quantity of dye was dissolved in distilled water to prepare a stock solution ($500\,mg\,L^{-1}$) – for AB113 and AB1 dyes. Experimental solutions of the desired concentrations were obtained by successive dilutions. The calibration curves for AB113 and AB1 were linear from 0.125 to 100 $mg\,L^{-1}$ ($R^2 = 0.999$) and 0.062 to 100 $mg\,L^{-1}$ ($R^2 = 0.999$). The adsorption equilibrium experiments were carried out in a batch process. The equilibrium isotherms were studied in 250 ml Erlenmeyer flasks housed in an incubator container. The synthetic dyes solutions were prepared by dissolving dyes in distilled water to produce a solution of $150\,mg\,L^{-1}$ of each dye. To determine the equilibrium time of AB113 and AB1 adsorption onto GPAC, an accurate amount of GPAC of 0.12 g was added to two Erlenmeyer flasks with $250\,cm^3$ volume containing 250 ml of each dye solution ($150\,mg\,L^{-1}$). The contents of flasks were mixed using a magnetic stirrer and 1 ml samples were taken at regular times. The equilibrium times for AB113 and AB1 were determined to be 250 and 167 h, respectively. Accurately weighed amounts of GAC sorbent of 0.01, 0.02 and 0.2 g increments to 0.2 g for AB113 and 0.01, 0.02 and 0.2 g increments to 0.18 g were added to each flask with 250 ml dye solution ($150\,mg\,L^{-1}$) at pH 7.4 ± 0.2 for AB113 and 7.0 ± 0.2 for AB1 dyes. The pH values at the end of batch runs were 6.1 ± 0.2 and 5.9 ± 0.2 for AB113 and AB1 dyes, respectively. The content of all Erlenmeyer flasks were mixed thoroughly for 250 and 167 h for AB113 and AB1 respectively at 20.3 °C using magnetic stirrers at constant revolution. A 5 ml sample was taken after the equilibrium time and centrifuged at 3800 rpm for 5 min. Then the dye concentration in the samples was measured spectrophotometrically.

The 250 ppm concentration dye solutions for AB80, AR114 and AY117 dyes were used to determine the equilibrium contact time. For each acid dye system, eight jars of fixed volume ($0.05\,dm^3$) of dye solutions were prepared and contacted with 0.05 g activated carbon F400. Then, the jars were put into the shaking bath with the same conditions of the isotherm adsorption experiment (constant temperature 20 °C and 200 rev/min shaking rate). At 3-day intervals, one of the jars was taken from the shaker and the dye concentration was measured. By plotting the acid dye adsorption capacity of the activated carbon against the time, it was found that the activated carbon adsorption capacity became constant after a certain period of time. It implied that the dye adsorption system had reached equilibrium at that time. Therefore, the equilibrium contact time can be determined from the graph. The activated carbon adsorption capacity of all three acid dyes (AB80, AR114 and AY117) in the samples became constant after 21 days. The equilibrium contact time for the sorption equilibrium studies has been shown to be 21 days minimum [23].

The amount of dye adsorbed onto the sorbent, was calculated as follows:

$$q_e = \frac{(C_0 - C_e)V}{m} \quad (1)$$

Each isotherm study were repeated three times and the mean values have been reported.

2.5. Determining isotherm parameters by non-linear regression

Due to the inherent bias resulting from linearization, alternative isotherm parameter sets were determined by non-linear regression. This provides a mathematically rigorous method for determining isotherm parameters using the original form of the isotherm equation [26–29]. Non-linear analysis of isotherm data is an interesting mathematical approach for describing adsorption isotherms at a constant temperature for water and wastewater treatment applications and to predict the overall sorption behavior under different operating conditions. Indeed, as different forms of the equation affected R^2 values more significantly during the linear analysis, the non-linear analysis might be a method of avoiding such errors [30]. Most commonly, algorithms based on the Levenberg–Marquardt or Gauss–Newton methods [31–33] are used.

The optimization procedure requires the selection of an error function in order to evaluate the fit of the isotherm to the exper-

imental equilibrium data. The choice of error function can affect the parameters derived-error functions based primarily on absolute deviation bias the fit towards high concentration data and this weighting increases when the square of the deviation is used to penalize extreme errors. This bias can be offset partly by dividing the deviation by the measured value in order to emphasize the significance of fractional deviations. In this study, nine non-linear error functions were examined and in each case a set of isotherm parameters were determined by minimizing the respective error function across the concentration range studied. The error functions employed were as follows:

1. Residual root mean square error (RMSE):

$$\sqrt{\frac{1}{n-2}\sum_{i=1}^{N}(q_{e,exp}-q_{e,cal})^2} \tag{2}$$

2. The chi-square test [32] is given as:

$$\chi^2=\sum_{i=1}^{N}\frac{(q_{e,exp}-q_{e,calc})^2}{q_{e,calc}} \tag{3}$$

If data from the model are similar to the experimental data, χ^2 will be a small number; if they are different, χ^2 will be a large number. The subscripts "exp" and "calc" show the experimental and calculated values and N is the number of observations in the experimental data. The smaller the RMSE value, the better the curve fitting [34].

3. The G^2-test statistic is calculated by taking an observed number (q_{exp}), dividing it by the predicted number (q_m), then taking the natural logarithm of this ratio. The test statistic is usually called G^2, and thus this is a G^2-test, although it is also sometimes called a log-likelihood test or a likelihood ratio test. The equation is:

$$G^2=2\sum_{i}^{N}\left[q_{exp,i}\times\ln\left(\frac{q_{exp,i}}{q_{m,i}}\right)\right] \tag{4}$$

The natural logarithm of 1 is 0; if the observed number is larger than the expected, $\ln(q_{exp}/q_m)$ is positive, while if q_{exp} is less than q_m, $\ln(q_{exp}/q_m)$ is negative. Each logarithm is multiplied by the observed number, and then these products are summed and multiplied by two. As with most test statistics, the larger the difference between observed and expected, the larger the test statistic becomes. The distribution of the G^2-statistic under the null hypothesis is approximately the same as the theoretical chi-square distribution. This means that once the G-statistic known; the probability of getting that value of G can be calculated using the chi-square distribution. The shape of the chi-square distribution depends on the number of degrees of freedom. The number of degrees of freedom is simply the number of experimental data points (N), minus the number of model parameters [35,36].

4. The sum of the squares of the errors (ERRSQ):

$$\sum_{i=1}^{N}(q_{e,exp}-q_{e,calc})_i^2 \tag{5}$$

5. A composite fractional error function (HYBRD):

$$\sum_{i=1}^{N}\left[\frac{(q_{e,exp}-q_{e,calc})^2}{q_{e,exp}}\right]_i \tag{6}$$

6. A derivative of Marquardt's percent standard deviation (MPSD) [37]:

$$\sum_{i=1}^{N}\left[\frac{(q_{e,exp}-q_{e,calc})}{q_{e,exp}}\right]_i^2 \tag{7}$$

7. The average relative error (ARE) [38]:

$$\sum_{i=1}^{N}\left|\frac{q_{e,exp}-q_{e,calc}}{q_{e,exp}}\right|_i \tag{8}$$

8. The sum of the absolute errors (EABS):

$$\sum_{i=1}^{N}\left|q_{e,exp}-q_{e,calc}\right|_i \tag{9}$$

9. The average percentage errors (APE):

$$\frac{\sum_{i=1}^{N}\left|(q_{e,exp}-q_{e,calc})/q_{e,exp}\right|_i}{N}\times 100 \tag{10}$$

10. Second-order corrected Akaike information criterion (AIC_C):

The AIC methodology [39] attempts to find the model that best explains the data with a minimum number of free parameters. Assuming that model errors are normally and independently distributed. The AIC is defined by the following equation:

$$AIC=N\ \ln\left(\frac{RSS}{N}\right)+2P \tag{11}$$

where P is the number of parameters in the model, and N the number of data points.

The preferred model is the one with the lowest AIC value.

When N is small compared to P, the second-order corrected AIC value (AIC_C) is more accurate:

$$AIC_C=AIC+\frac{2P(P+1)}{N-P-1} \tag{12}$$

11. Mallows CP statistic (CP):

Mallows [40] developed a method to find adequate models by plotting a special statistic against the number of variables +1. CP statistic can calculate as below:

$$\frac{SS_{res}}{RMSE}-N+(2\times P) \tag{13}$$

where SS_{res} is the residual sum of squares for the model with $P-1$ variables, RMSE is the residual mean square when using all available variables, N is the number of observations, and P is the number of variables used for the model plus one.

The general procedure to find an adequate model by means of the CP statistic is to calculate CP for all possible combinations of variables and the CP values against P. The model with the lowest CP value approximately equal to P is the most "adequate" model. As each of the error criteria is likely to produce a different set of isotherm parameters, an overall optimum parameter set is difficult to identify directly. Hence, in order to try to make a meaningful comparison between the parameter sets, a procedure of normalizing and combining the error results was adopted producing a so-called 'sum of the normalized errors' for each parameter set for each isotherm.

The calculation method for the 'sum of the normalized errors' was as follows:

(a) Select one isotherm and one error function and determine the isotherm parameters that minimize that error function for that

Table 3
The names and non-linear forms of studied isotherm models.

Isotherm	Non-linear form	
Langmuir	$q_e = \frac{q_m b C_e}{1 + bC_e}$	(14)
Freundlich	$q_e = k_f C_e^{1/n}$	(15)
Dubinin–Radushkevich	$q_e = Q_s \exp(-B_D \varepsilon^2)$	(16)
	$\varepsilon = RT \ln\left(1 + \frac{1}{C_e}\right)$	(17)
Jovanovic	$q_e = q_{max}(1 - e^{(K_j C_e)})$	(18)
Harkins–Jura	$q_e = \left(\frac{A}{B_2 - \log C_e}\right)^{1/2}$	(19)
Halsey	$q_e = \exp\left(\frac{\ln K_H - \ln C_e}{n}\right)$	(20)
Temkin	$q_e = \frac{RT}{b_T} \ln(K_T C_e)$	(21)

isotherm to produce the isotherm parameter set for that error function,
(b) Determine the values for all the other error functions for that isotherm parameter set,
(c) Calculate all other parameter sets and all their associated error function values for that isotherm,
(d) Select each error measure in turn and ratio the value of that error measure for a given parameter set to the largest value of that error from all the parameter sets for that isotherm, and
(e) Sum all these normalized errors for each parameter set.

The parameter set thus providing the smallest normalized error sum can be considered to be optimal for that isotherm provided:

- There is no bias in the data sampling – i.e. the experimental data are evenly distributed, providing an approximately equal number of points in each concentration range, and
- There is no bias in the type of error methods selected.

3. Results and discussion

3.1. Adsorption isotherms

In general, the adsorption isotherm describes how adsorbates interact with adsorbents and therefore it is critical in optimizing the use of adsorbents. The studied isotherms non-linear forms equations are shown in Table 3.

The Langmuir [9,41] equation is valid for monolayer sorption onto a surface with a finite number of identical sites. Fig. 1 shows

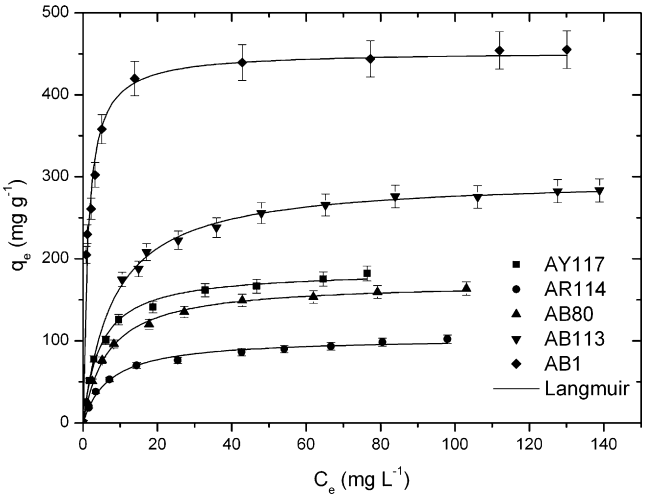

Fig. 1. Comparison of experimental and predicted adsorption isotherms of acid dyes onto GPAC (AB1 and AB113 dyes) and activated carbon F400 (AY117, AR114 and AB80 dyes) according to Langmuir model.

the theoretical and experimental adsorption data according to the Langmuir model and the values of the isotherm parameters and related error functions values are shown in Tables 4 and 5, respectively. The values of maximum adsorption capacity determined using Langmuir model was 298.4, 452.9, 171.5, 103.7 and 185.8 for AB113, AB1, AB80, AR114 and AY117 dyes, respectively. These values are near the experimental adsorbed amounts and correspond closely to the adsorption isotherm plateau, which are acceptable.

The essential characteristics of the Langmuir isotherm can be expressed in terms of dimensionless constant separation factor or equilibrium parameter, R_L [42] which is defined by Eq. (22):

$$R_L = \frac{1}{1 + bC_0} \quad (22)$$

where b and C_0 (mg L^{-1}) are the Langmuir constant and the highest initial dye concentration respectively. According to the value of R_L the isotherm shape can be interpreted as follows (Table 3). The dimensionless separation factors calculated for AB113, AB1, AB80, AR114 and AY117 were found to be 2.23×10^{-5}, 1.47×10^{-5}, 2.33×10^{-5}, 3.86×10^{-5}, and 2.15×10^{-5}, respectively. The R_L values are less than 1 and greater than 0 indicating very favorable adsorption.

The empirical Freundlich [6] equation is based on sorption onto a heterogeneous surface. The magnitude of exponent n gives

Table 4
Isotherm parameters, χ^2 and G^2 statistics of two-parameter models.

Model	Parameter	AB113	AB1	AB80	AR114	AY117
Jovanovic	q_{mj}	271.4	433.7	152.4	92.2	167.1
	K_j	0.081	0.492	0.120	0.114	0.166
Temkin	K_T	6.89	126.9	2.03	1.99	3.50
	b_T	57.37	49.31	75.71	125.40	73.54
Harkins–Jura	A_H	177600	544200	27560	9857	31220
	B	6.97	7.19	5.48	5.4	5.14
Dubinin–Radushkevich	q_d	269.4	417.5	145.3	88.5	158.3
	B_d	0.028	0.001	0.006	0.007	0.003
Freundlich	K_f	124.2	253.5	46.9	28.0	56.9
	n	5.74	7.57	3.47	3.44	3.53
Halsey	K_H	0.000	0.000	0.000	0.000	0.000
	n	−5.74	−7.57	−3.47	−3.44	−3.53
Langmuir	q_m	298.4	452.9	171.4	103.7	185.8
	b	0.12	0.79	0.15	0.14	0.22

Table 5
Values of the error functions of the two-parameter isotherm models.

Dye	Error function Model	Isotherm model						
		Langmuir	Freundlich	Harkins	Temkin	Jovanovic	Dubinin	Halsey
AB113	G^2	1.89	1.91	1550	1.99	17.41	13.27	1.90
	χ^2	0.83	3.40	266.8	1.98	6.41	9.84	3.40
	RMSE	4.17	8.85	70.69	6.82	11.81	14.56	8.85
	HYBRD	0.83	3.46	187.1	2.0	6.28	9.68	3.46
	MPSD	0.004	0.016	0.705	0.009	0.029	0.046	0.016
	ARE	0.168	0.376	2.534	0.291	0.462	0.599	0.376
	APE (%)	1.40	3.13	21.11	2.43	3.85	4.99	3.13
	Mallows	33.69	80.52	698.9	60.21	110.1	137.6	80.52
	AIC_C	37.41	105.3	105.3	49.22	62.40	67.43	55.48
	p value G^2	0.9971	0.9969	0.0000	0.9964	0.06573	0.2088	0.9970
	p value χ^2	0.9999	0.9702	0.0000	0.9964	0.7798	0.4544	0.9702
AB1	G^2	26.32	20.45	1423	18.94	135.9	83.12	20.41
	χ^2	8.907	32.13	292.8	19.25	48.71	57.88	32.14
	RMSE	15.52	33.93	100.7	26.92	34.34	44.58	33.93
	HYBRD	8.673	31.86	226.4	18.44	40.90	60.68	31.87
	MPSD	0.036	0.109	0.602	0.057	0.167	0.219	0.109
	ARE	0.422	0.861	2.282	0.651	0.985	1.186	0.861
	APE (%)	3.836	7.827	20.75	5.917	8.959	10.78	7.827
	Mallows	132.7	298.4	899.3	235.3	302.1	394.3	298.4
	AIC_C	63.62	104.8	104.8	75.74	81.09	86.46	80.83
	p value G^2	0.0018	0.0153	0.0000	0.0256	0.0000	0.0000	0.0155
	p value χ^2	0.4459	0.0001	0.0000	0.0231	0.0000	0.0000	0.0001
AB80	G^2	1.05	8.70	914.4	3.22	30.75	212.6	8.59
	χ^2	1.11	21.94	317.4	3.11	7.53	630.5	21.95
	RMSE	2.78	13.40	54.54	5.38	8.68	17.97	13.40
	HYBRD	1.16	36.69	263.3	3.50	6.94	49.71	36.74
	MPSD	0.030	1.262	5.114	0.091	0.093	1.306	1.265
	ARE	0.355	1.815	5.094	0.592	0.741	2.365	1.816
	APE (%)	3.22	16.50	46.31	5.38	6.73	21.50	16.51
	Mallows	18.04	113.6	483.8	41.48	71.11	154.8	113.6
	AIC_C	25.80	91.27	91.27	40.34	50.83	66.85	60.39
	p value G^2	0.9993	0.4651	0.0000	0.9546	0.0003	0.0000	0.4756
	p value χ^2	0.9991	0.0090	0.0000	0.9596	0.5818	0.0000	0.0090
AR114	G^2	3.97	2.62	634.6	1.03	22.01	100.9	2.58
	χ^2	1.33	7.96	205.8	1.01	6.64	183.3	7.96
	RMSE	3.21	6.06	34.33	2.18	6.60	11.10	6.06
	HYBRD	1.29	11.87	143.9	1.09	6.10	27.17	11.88
	MPSD	0.021	0.56	3.08	0.042	0.126	1.018	0.561
	ARE	0.354	1.149	4.520	0.347	0.902	2.010	1.149
	APE (%)	3.22	10.44	41.09	3.15	8.20	18.28	10.44
	Mallows	21.91	47.58	302.0	12.61	52.48	92.87	47.58
	AIC_C	28.97	81.09	81.09	20.43	44.84	56.24	42.95
	p value G^2	0.9130	0.9772	0.0000	0.9993	0.0088	0.0000	0.9786
	p value χ^2	0.9982	0.5378	0.0000	0.9994	0.6745	0.0000	0.5375
AY117	G^2	12.56	5.31	951.5	2.42	55.32	348.2	5.232
	χ^2	2.48	20.83	336.8	2.38	16.07	9378	20.84
	RMSE	4.80	13.21	58.75	4.96	11.22	20.09	13.21
	HYBRD	2.30	31.45	285.8	2.51	13.00	53.29	31.49
	MPSD	0.043	0.971	5.360	0.037	0.247	1.316	0.972
	ARE	0.448	1.691	5.205	0.405	1.156	2.285	1.691
	APE (%)	4.07	15.37	47.31	3.68	10.51	20.77	15.38
	Mallows	36.28	111.9	521.7	37.70	94.01	173.8	111.9
	AIC_C	37.84	92.90	92.90	38.55	56.49	69.30	60.07
	p value G^2	0.1834	0.8063	0.0000	0.9830	0.0000	0.0000	0.8137
	p value χ^2	0.9815	0.0134	0.0000	0.9839	0.0654	0.0000	0.0133

an indication on the favorability of adsorption. It is generally stated that the values n in the range of 2–10 represent good, 1–2 moderately difficult and less than 1 poor adsorption characteristics. The adsorption isotherms and constant parameters of the isotherm equations were calculated by non-linear trial-and-error method. Fig. 2 shows the theoretical and experimental adsorption data according to the Freundlich model and the values of the isotherm parameters and related error functions values are shown in Tables 4 and 5, respectively. As shown, the Freundlich isotherm generated a satisfactory fit to the experimental data as indicated by the error functions. However, the Langmuir isotherm shows a better fit to the adsorption data than the Freundlich isotherm in the sorption of AB1, AB113 and AB80 dyes. Such a trend is quite logical since the Freundlich equation is a pure exponential one, which means that when $C_e \sim \infty$, q_e will also extend to ∞ [43]. However, for all dyes adsorption systems, since there is a clear saturation plateau, the calculated q_e will necessary tend towards a constant (i.e. maximum adsorption capacity). The fact that the Langmuir isotherm fits the experimental data well may be due to the predominantly homogeneous distribution of active sites on the activated carbons surface; since the Langmuir equation assumes that the adsorbent surface is energetically homogeneous [7]. It is apparent that the value of Freundlich constant, n, obtained indicates favorable adsorption, as it is equal to 5.74, 7.57, 3.47, 3.44

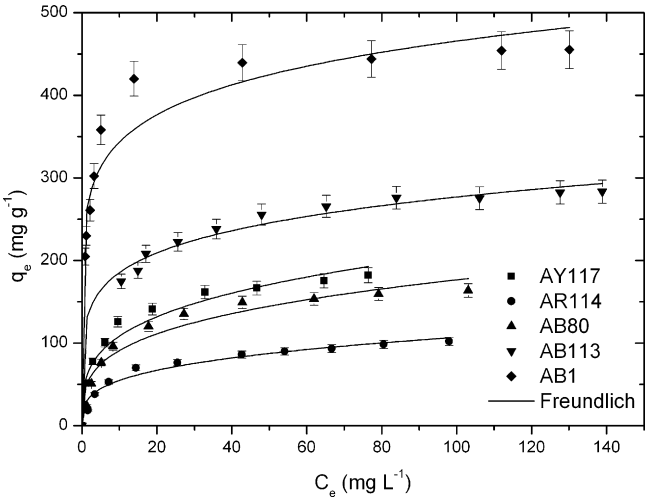

Fig. 2. Comparison of experimental and predicted adsorption isotherms of acid dyes onto GPAC (AB1 and AB113 dyes) and activated carbon F400 (AY117, AR114 and AB80 dyes) according to Freundlich model.

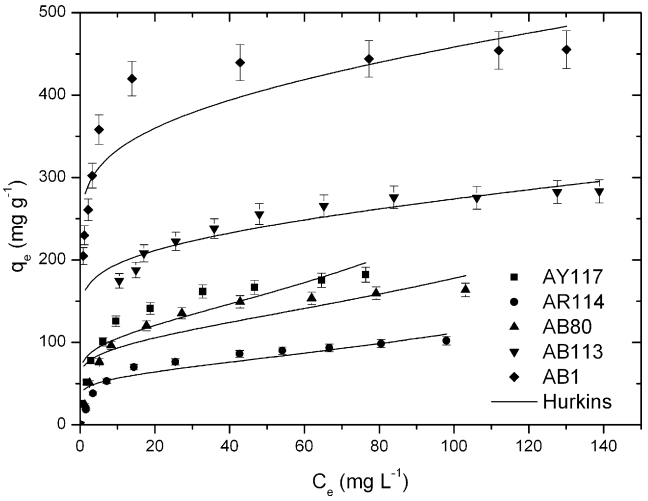

Fig. 4. Comparison of experimental and predicted adsorption isotherms of acid dyes onto GPAC (AB1 and AB113 dyes) and activated carbon F400 (AY117, AR114 and AB80 dyes) according to Harkins–Jura model.

and 3.53 for AB113, AB1, AB80, AR114 and AY117 dyes, respectively.

Temkin and Pyzhev [8] studied the heat of adsorption and the adsorbent–adsorbate interaction on surfaces. The variation of adsorption energy, b_T, is positive for all dyes and was obtained 57.4 49.3, 75.7, 125.4, and 73.5 for AB113, AB1, AB80, AR114 and AY117 dyes, respectively. These indicate the adsorption reaction is exothermic. The theoretical isotherm curves are compared with the corresponding experimental data in Fig. 3 and the obtained error function values are presented in Table 5. The experimental equilibrium curves are close to those predicted by the Temkin model. Consequently, the Temkin isotherm cannot describe the adsorption isotherms of acid dyes onto activated carbons acceptably. For AB113, AB1, and AB80 the Temkin model after Langmuir model could describe experimental isotherm results acceptably. For AB114 and AB117 dyes the Temkin model describes the experimental data better than Langmuir model.

The Harkins–Jura [12] adsorption isotherm accounts for multilayer adsorption and can be explained by the existence of a heterogeneous pore distribution. The theoretical and experimental isotherm data according to Harkins–Jura isotherm model for the sorption of acid dyes onto activated carbons are shown in Fig. 4. According to the obtained error functions in Table 5, this model shows the poorest agreement with experimental data and this result indicate adsorption of acidic dyes onto activated carbon cannot be described by the assumptions of Harkins–Jura model.

The Halsey [11] adsorption isotherm is suitable for multilayer adsorption and the fitting of the experimental data to this equation attest to the heteroporous nature of the adsorbent. Relatively poor agreement was found for the Halsey model with the isotherm data. As shown in Fig. 5 this model provides better agreement with experimental data in the sorption of AB113 and AB1 dyes in comparison with other dyes.

Radushkevich [44] and Dubinin [45] have reported that the characteristic sorption curve is related to the porous structure of the sorbent. Comparison of experimental and predicted adsorption isotherms of acid dyes onto activated carbons according to the Dubinin model shown in Fig. 6. The constant, B_D, is related to the mean free energy of sorption per mole of the sorbate as it is transferred to the surface of the solid from an infinite distance in the solution. The values of theoretical monolayer saturation capacity in the Dubinin model obtained using non-linear regression (Table 4)

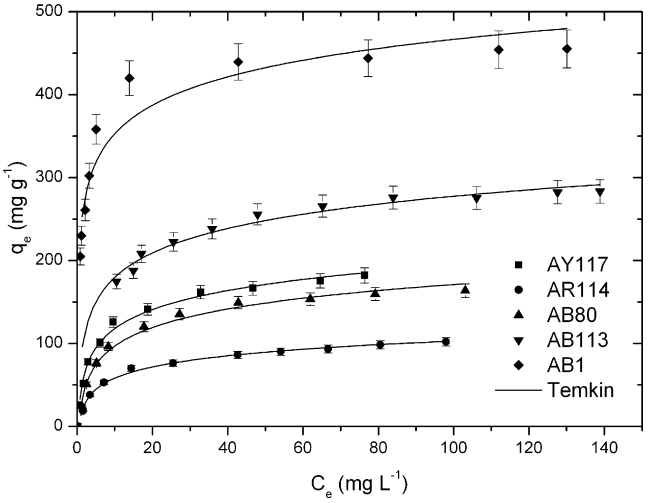

Fig. 3. Comparison of experimental and predicted adsorption isotherms of acid dyes onto GPAC (AB1 and AB113 dyes) and activated carbon F400 (AY117, AR114 and AB80 dyes) according to Temkin model.

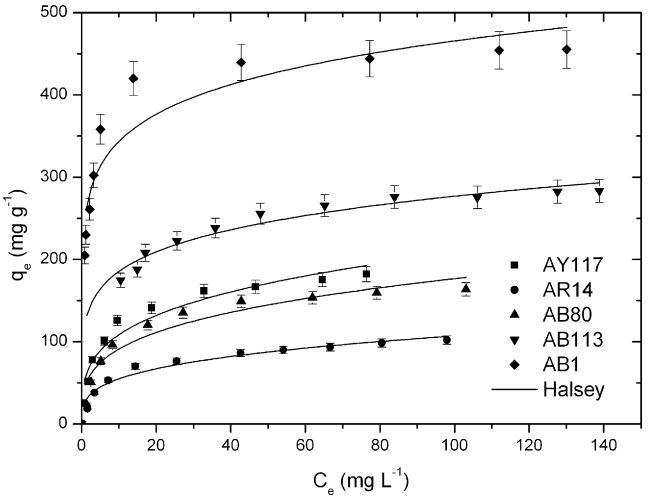

Fig. 5. Comparison of experimental and predicted adsorption isotherms of acid dyes onto GPAC (AB1 and AB113 dyes) and activated carbon F400 (AY117, AR114 and AB80 dyes) according to Halsey model.

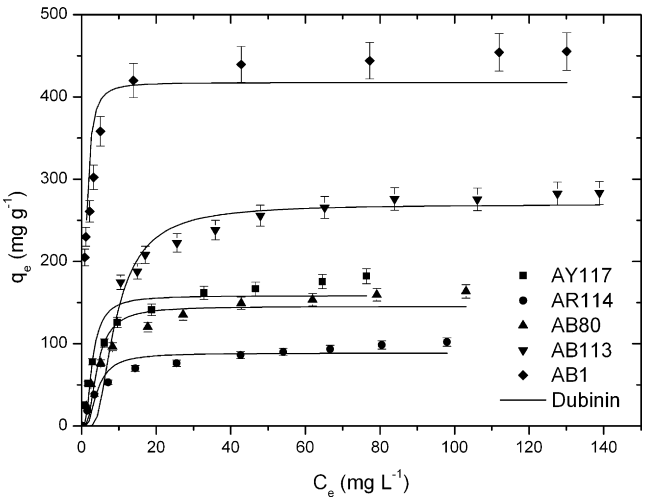

Fig. 6. Comparison of experimental and predicted adsorption isotherms of acid dyes onto GPAC (AB1 and AB113 dyes) and activated carbon F400 (AY117, AR114 and AB80 dyes) according to Dubinin–Radushkevich model.

are lower than the experimental amounts corresponding to the adsorption isotherm plateau, which is unacceptable.

The model of an adsorption surface considered by Jovanovic [9] is essentially the same as that considered by Langmuir, except that allowance is made in the former for the surface binding vibrations of an adsorbed species. The Jovanovic equation represents another approximation for monolayer localized adsorption without lateral interactions. The same kind of approximation leads to the result that monolayer adsorption of mobile hard discs is described by the Langmuir isotherm. The experimental and Jovanovic model data are shown in Fig. 7. The maximum adsorption capacities for studied dyes based on Jovanovic model (Table 4) were lower than Langmuir maximum adsorption monolayer capacities and the experimental amounts are correspond to the adsorption isotherm plateaus, which is unacceptable.

Over the past few decades, linear regression has been developed as a major option in designing the adsorption systems. However, recent investigations have indicated the growing discrepancy (between the predictions and experimental data) and disability of the model, propagating towards a different outcome. However the expanding of the non-linear isotherms represents a potentially

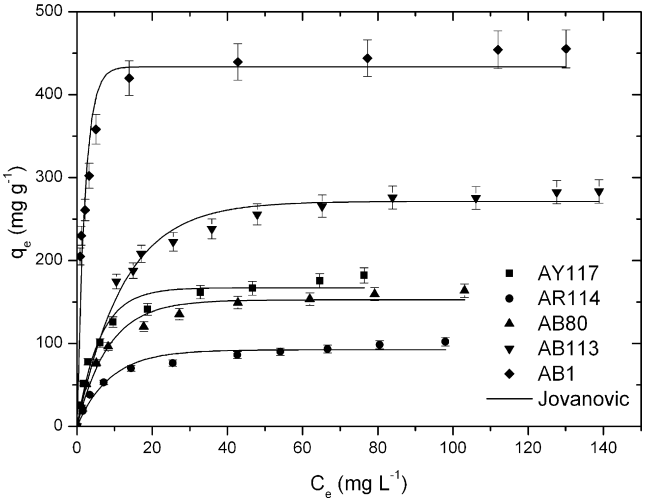

Fig. 7. Comparison of experimental and predicted adsorption isotherms of acid dyes onto GPAC (AB1 and AB113 dyes) and activated carbon F400 (AY117, AR114 and AB80 dyes) according to Jovanovic model.

Table 6
Isotherm model comparison.

Dye	Error function	Isotherm model comparison
AR114	G^2	Tem > Hal > Fre > La
	χ^2	Tem > La > Jo > Fre
	RMSE	Tem > La > Fre > Hal
	HYBRD	Tem > La > Jo > Fre
	MPSD	La > Tem > Jo > Fre
	ARE	Tem > La > Jo > Fre
	APE (%)	Tem > La > Jo > Fre
	Mallows	Tem > La > Fre > Jo
	AIC_C	Tem > La > Hal > Jov
AY117	G^2	Tem > Hal > Fre > La
	χ^2	Tem > La > Jo > Fre
	RMSE	La > Tem > Jo > Fre
	HYBRD	La > Tem > Jo > Fre
	MPSD	Tem > La > Jo > Fre
	ARE	Tem > La > Jo > Fre
	APE (%)	Tem > La > Jo > Fre
	Mallows	Tem > La > Fre > Jo
	AIC_C	La > Tem > Hal > Fre
AB80	G^2	La > Tem > Hal > Fre
	χ^2	La > Tem > Jo > Fre
	RMSE	La > Tem > Jo > Fre
	HYBRD	La > Tem > Jo > Fre
	MPSD	La > Tem > Jo > Fre
	ARE	La > Tem > Jo > Fre
	APE (%)	La > Tem > Jo > Fre
	Mallows	La > Tem > Jo > Fre
	AIC_C	La > Tem > Hal > Fre
AB1	G^2	Tem > Hal > Fre > La
	χ^2	La > Tem > Fre > Hal
	RMSE	La > Tem > Fre > Hal
	HYBRD	La > Tem > Fre > Hal
	MPSD	La > Tem > Fre > Hal
	ARE	La > Tem > Fre > Hal
	APE (%)	La > Tem > Fre > Hal
	Mallows	La > Tem > Fre > Hal
	AIC_C	La > Tem > Hal > Fre
AB113	G^2	La > Hal > Fre > Tem
	χ^2	La > Tem > Fre > Hal
	RMSE	La > Tem > Fre > Hal
	HYBRD	La > Tem > Fre > Hal
	MPSD	La > Tem > Fre > Hal
	ARE	La > Tem > Fre > Hal
	APE (%)	La > Tem > Fre > Hal
	Mallows	La > Tem > Fre > Hal
	AIC_C	La > Hal > Fre > Tem

viable and powerful tool, leading to the superior improvement in the area of adsorption science [46].

4. Conclusions

The orders of the isotherm model best fits are presented in Table 6. It is apparent that the Langmuir and the Temkin dominate, almost, exclusively, for all the error function selection methods.

There are some interesting features from the experimental data results and in Table 6:

(i) The adsorption capacities on the mesoporous pine-cone carbon are substantially higher than those on the commercial F400 microporous carbon;
(ii) The high dye capacity mesoporous adsorbents tend to be best modeled according to the Langmuir isotherm;
(iii) The lower capacity systems using molecular weight dyes on the microporous carbon favor the Temkin isotherm;
(iv) The smaller molecular mass dye adsorbing onto the microporous carbon is represented equally by the Langmuir and the Temkin isotherm models.

Acknowledgments

The authors thank the Hamadan University of medical sciences for financial support.

Appendix A. Supplementary data

Supplementary data associated with this article can be found, in the online version, at doi:10.1016/j.cej.2010.03.016.

References

[1] E. Forgacs, T. Cserhati, G. Oros, Removal of synthetic dyes from wastewaters: a review, Environ. Int. 30 (2004) 953–971.
[2] T. Robinson, G. McMullan, R. Marchant, P. Nigam, Remediation of dyes in textile effluent: a critical review on current treatment technologies with a proposed alternative, Bioresour. Technol. 77 (2001) 247–255.
[3] S. Venkat Mohan, S. Krishna Mohan, J. Karthikeyan, Adsorption mechanism of acid-azo dye from aqueous solution on to coal/coal based sorbents and activated carbon: a mechanist study, in: S. Jayarama Reddy (Ed.), Analytical Techniques in Monitoring the Environment, vol. 97, Student Offset Printers, Tirupathi, India, 2000, pp. 97–103.
[4] K.K.H. Choy, J.F. Porter, G. McKay, Comparison of solutions for the homogeneous surface diffusion model applied to adsorption systems, Chem. Eng. J. 98 (2004) 255–264.
[5] K.K.H. Choy, J.F. Porter, G. McKay, Intraparticle diffusion in single and multicomponent acid dye adsorption from wastewater onto carbon, Chem. Eng. J. 103 (2004) 133–145.
[6] H.Z. Freundlich, Over the adsorption in solution, J. Phys. Chem. 57A (1906) 385–397.
[7] I. Langmuir, The adsorption of gases on plane surfaces of glass, mica, and platinum, J. Am. Chem. Soc. 40 (1918) 1361–1403.
[8] M.J. Temkin, V. Pyzhev, Kinetics of ammonia synthesis on promoted iron catalysts, Acta Physiochim. URSS 12 (1940) 217–222.
[9] M.M. Dubinin, L.V. Radushkevich, The equation of the characteristic curve of activated charcoal, Dokl. Akad. Nauk. SSSR 55 (1947) 327–329.
[10] D.S. Jovanovic, Physical adsorption of gases. I. Isotherms for monolayer and multilayer adsorption, Colloid Polym. Sci. 235 (1969) 1203–1214.
[11] G. Halsey, Physical adsorption on nonuniform surfaces, J. Chem. Phys. 16 (1948) 931–937.
[12] W.D. Harkins, E.J. Jura, The decrease of free surface energy as a basis for the development of equations for adsorption isotherms; and the existence of two condensed phases in films on solids, J. Chem. Phys. 12 (1944) 112–113.
[13] M.M. Nassar, M.S. El-Geundi, Comparative cost of colour removal from textile effluents using natural adsorbents, J. Chem. Technol. Biotechnol. 50 (1991) 257–264.
[14] C. Grégorio, Non-conventional low-cost adsorbents for dye removal: a review, Bioresour. Technol. 97 (2006) 1061–1067.
[15] G. McKay, G. Ramprasad, P. Pratapa-Mowli, Desorption and regeneration of dye colours from low cost materials, Water Res. 21 (3) (1987) 375–377.
[16] M. Valix, W.H. Cheung, G. McKay, Roles of the textural and surface chemical properties of activated carbon in the adsorption of acid blue dye, Langmuir 22 (2006) 4574–4582.
[17] Y.S. Ho, G. McKay, Kinetic models for the sorption of dye from aqueous solution by wood, Trans. IChemE. 76 (Part B) (1998) 183–191.
[18] Y.S. Ho, T.H. Chiang, Y.M. Hsueh, Removal of basic dye from aqueous solution using tree fern as a biosorbent, Process. Biochem. 40 (1) (2005) 119–124.
[19] Y.S. Ho, W.T. Chiu, C.W. Chung, Regression analysis for the sorption isotherms of basic dyes on sugarcane dust, Bioresour. Technol. 96 (11) (2005) 1285–1291.
[20] M. Arami, et al., Removal of dyes from colored textile wastewater by orange peel adsorbent: equilibrium and kinetic studies, J. Colloid Interface Sci. 228 (2) (2005) 371–376.
[21] S.J. Allen, G. McKay, J.F. Porter, Adsorption isotherm models for basic dye adsorption by peat in single and binary component systems, J. Colloid Interface Sci. 280 (2004) 322–333.
[22] G. McKay, H.S. Blair, J.R. Gardner, Two resistance mass transport model for the adsorption of acid dye onto chitin in fixed beds, J. Appl. Polym. Sci. 33 (1987) 1249–1257.
[23] K.K.H. Choy, J.P. Porter, G. McKay, Single and multicomponent equilibrium studies for the adsorption of acidic dyes on carbon from effluents, Langmuir 20 (2004) 9646–9656.
[24] L. Noszko, et al., Preparation of activated carbon from the by-products of agricultural industry, Period. Polytech. Chem. Eng. 28 (1984) 293–297.
[25] ASTM D4607-94, Standard Test Method for Determination of Iodine Number of Activated Carbon, 1999.
[26] A.R. Khan, I.R. Al-Waheab, A. Al-Haddad, A generalized equation for adsorption isotherms for multi-component organic pollutants in dilute aqueous solution, Environ. Technol. 17 (1996) 13–23.
[27] A. Malek, S. Farooq, Comparison of isotherm models for hydrocarbon adsorption on activated carbon, AIChE. J. 42 (1996) 431–441.
[28] A. Seidel, D. Gelbin, On applying the ideal adsorbed solution theory to multicomponent adsorption equilibria of dissolved organic components on activated carbon, Chem. Eng. Sci. 43 (1988) 79–89.
[29] A. Seidel-Morgenstern, G. Guichon, Modelling of the competitive isotherms and the chromatographic separation of two enantiomers, Chem. Eng. Sci. 48 (1993) 2787–2797.
[30] M.C. Ncibi, Applicability of some statistical tools to predict optimum adsorption isotherm after linear and non-linear regression analysis, J. Hazard. Mater. 153 (2008) 207–212.
[31] T.F. Edgar, D.M. Himmelblau, Optimization of Chemical Processes, McGraw-Hill, New York, 1989.
[32] O.T. Hanna, O.C. Sandall, Computational Methods in Chemical Engineering, Prentice-Hall International, New Jersey, 1995.
[33] Y.S. Ho, Selection of optimum sorption isotherm, Carbon 42 (2004) 2115–2116.
[34] S.C. Tsai, K.W. Juang, Comparison of linear and non-linear forms of isotherm models for strontium sorption on a sodium bentonite, J. Radioanal. Nucl. Chem. 243 (2000) 741–746.
[35] A. Agresti, An Introduction to Categorical Data Analysis, 2nd ed., John Wiley & Sons Inc., Hoboken, NJ, 2007.
[36] H. Chernoff, E.L. Lehmann, The use of maximum likelihood estimates in χ^2 tests for goodness-of-fit, Ann. Math. Stat. 25 (1954) 579–584.
[37] D.W. Marquardt, An algorithm for least-squares estimation of nonlinear parameters, J. Soc. (Ind.) Appl. Math. 11 (1963) 431–441.
[38] A. Kapoor, R.T. Yang, Correlation of equilibrium adsorption data of condensable vapours on porous adsorbents, Gas Sep. Purif. (1989) 187–192.
[39] H. Akaike, A new look at the statistical model identification, IEEE Trans. Autom. Control 19 (6) (1974) 716–723.
[40] C.L. Mallows, Some comments on C_p, Technometrics 15 (1973) 661–662.
[41] K.K.H. Choy, J.F. Porter, G. McKay, Langmuir isotherm models applied to the multicomponent sorption of acid dyes from effluent onto activated carbon, Chem. Eng. J. 45 (2000) 575–584.
[42] K.R. Hall, et al., Pore and solid-diffusion kinetics in fixed-bed adsorption under constant-pattern conditions, Ind. Eng. Chem. Fund. 5 (2) (1966) 212–223.
[43] M.C. Ncibi, S. Altenor, M. Seffen, F. Brouers, S. Gaspard, Modelling single compound adsorption onto porous and non-porous sorbents using a deformed Weibull exponential isotherm, Chem. Eng. J. 145 (2008) 196–202.
[44] L.V. Radushkevich, Potential theory of sorption and structure of carbons, Zh. Fiz. Khim. 23 (1949) 1410–1420.
[45] M.M. Dubinin, Modern state of the theory of volume filling of micropore adsorbents during adsorption of gases and steams on carbon adsorbents, Zh. Fiz. Khim. 39 (1965) 1305–1317.
[46] K.Y. Foo, B.H. Hameed, Insights into the modeling of adsorption isotherm systems, Chem. Eng. J. 156 (2010) 2–10.